Cell

Second Cistron in *CACNA1A* Gene Encodes a Transcription Factor Mediating Cerebellar Development and SCA6

Xiaofei Du,[1] Jun Wang,[1] Haipeng Zhu,[1] Lorenzo Rinaldo,[2] Kay-Marie Lamar,[1] Ann C. Palmenberg,[3] Christian Hansel,[2] and Christopher M. Gomez[1,*]
[1]Department of Neurology
[2]Department of Neurobiology
University of Chicago, Chicago, IL 60637, USA
[3]Institute for Molecular Virology, University of Wisconsin-Madison, Madison, WI 53706, USA
*Correspondence: cgomez@neurology.bsd.uchicago.edu
http://dx.doi.org/10.1016/j.cell.2013.05.059

SUMMARY

The *CACNA1A* gene, encoding the voltage-gated calcium channel subunit α1A, is involved in pre- and postsynaptic Ca^{2+} signaling, gene expression, and several genetic neurological disorders. We found that *CACNA1A* coordinates gene expression using a bicistronic mRNA bearing a cryptic internal ribosomal entry site (IRES). The first cistron encodes the well-characterized α1A subunit. The second expresses a transcription factor, α1ACT, which coordinates expression of a program of genes involved in neural and Purkinje cell development. α1ACT also contains the polyglutamine (polyQ) tract that, when expanded, causes spinocerebellar ataxia type 6 (SCA6). When expressed as an independent polypeptide, α1ACT—bearing an expanded polyQ tract—lacks transcription factor function and neurite outgrowth properties, causes cell death in culture, and leads to ataxia and cerebellar atrophy in transgenic mice. Suppression of *CACNA1A* IRES function in SCA6 may be a potential therapeutic strategy.

INTRODUCTION

Voltage-gated calcium channel genes encode a large family of channel proteins (α1 subunits) that play critical roles in neuronal excitability, transmitter release, muscle contractility, and gene expression (Catterall, 2011). Genetic defects of these channels have been implicated in a variety of neurological, cardiac, and skeletal muscle disorders (Cain and Snutch, 2011). Diverse mutations in the α1A subunit, *CACNA1A* gene, causing either loss or gain of P/Q-type channel function, have been associated with dominantly inherited conditions of migraine, epilepsy, and episodic and progressive ataxia (Rajakulendran et al., 2012). The recognition that spinocerebellar ataxia type 6 (SCA6) is due to expansion of a polyglutamine (polyQ) tract encoded by a newly identified 47th exon in *CACNA1A*, from a normal range of Q4–Q17 to a pathological range of Q19–Q33, added further complexity to modeling both channel function and disease pathogenesis (Zhuchenko et al., 1997).

Attempts to attribute SCA6 to a disturbance in P/Q-type channel function associated with the expanded polyQ in the α1A subunit in heterologous expression systems have led to contradictory results, whereas two knockin studies showed no effect of expanded polyQ tracts on P/Q channel gating (Saegusa et al., 2007; Watase et al., 2008). Several laboratories have shown that the C terminus of the α1A subunit (α1ACT), which contains the polyQ tract, is present as a stable fragment in cultured cells or cerebellar tissues (Ishiguro et al., 2010; Kordasiewicz et al., 2006; Kubodera et al., 2003; Marquèze-Pouey et al., 2008; Scott et al., 1998) and enriched in cerebellar nuclei, based on nuclear localization signals in the α1ACT sequence (Kordasiewicz et al., 2006). This finding is similar to that of the C-terminal fragment of the L-type subunit that is translocated to the nucleus and functions as a transcription factor (Gomez-Ospina et al., 2006). Finally, the α1ACT fragment bearing SCA6-expanded polyQs is toxic to cultured cells and primary neurons (Ishiguro et al., 2010; Kordasiewicz et al., 2006; Kubodera et al., 2003; Marquèze-Pouey et al., 2008).

Here, we explored the origin and function of the α1ACT polypeptide in physiology and disease. We demonstrate that α1ACT is generated from the full-length α1A transcript by means of a cellular internal ribosomal entry site (IRES) located within the α1A messenger RNA (mRNA), i.e., that the *CACNA1A* gene is bicistronic. The α1ACT protein containing the normal polyQ tract is a transcription factor that binds and enhances expression of several Purkinje cell (PC)-expressed genes, promotes neurite outgrowth, and partially rescues the *CACNA1A* knockout phenotype. α1ACT with expanded polyQ has altered function, reduces viability of cells in vitro, and causes gait impairment and cerebellar cortical atrophy in vivo. We identify a truly bicistronic, dual-function cellular gene encoding two proteins with completely distinct functions: in this case, an ion channel and a transcription factor. This gene expression strategy demonstrates a role for an IRES in coordinating gene expression as well as a potential therapeutic target for disease-modifying therapy.

RESULTS

Identification of the C-Terminal Fragment of the *CACNA1A*-Encoded α1A Subunit

To identify the N-terminal sequence of the α1ACT fragment, we tagged the full-length human α1A subunit complementary DNA (cDNA) bearing normal polyQ (Q11), $\alpha1A_{WT}$, at its 3′ end with a 3xFLAG epitope and established HEK293 cell lines stably expressing this ~220 kDa α1A-FLAG fusion protein. The cell line grew normally and stably expressed the 75 kDa α1ACT-FLAG fusion protein. We affinity purified α1ACT-FLAG from the whole-cell lysate in a two-step procedure. Peak elution fractions (Figure 1A) collected from anion exchange chromatography (HiTrap DEAE FF) were subjected to affinity purification using anti-FLAG M2 magnetic beads. The isolated α1ACT fragment protein was seen as a unique 75 kDa band (arrowhead) above the heavy-chain immunoglobulin G (IgG) band on a Coomassie-stained SDS-PAGE gel (Figures 1B and 1C). Liquid chromatography-tandem mass spectrometry (LC-MS/MS) analysis of in-gel digest protein (The Rockefeller University Protein Resource Center) revealed that the amino acid sequence of N terminus of α1ACT fragment was Met Ile Met Glu Tyr (amino acids 1,960–1,964, nucleotides 6,114–6,128, GenBank accession numbers 187828892 and NM_001127222) (Figure 1D; Figure S1 available online). This sequence, which begins within the IQ-like domain of the full-length α1A subunit and does not overlap with any known protease cleavage site, is a highly homologous sequence in all vertebrate species (Wilkins et al., 1999).

To investigate the origin of the α1ACT protein fragment, we generated a series of constructs bearing different mutations of the α1A cDNA, as defined in Figure 1E, and transfected them into HEK293 cells. Deletion of 534 bps (α1Adel534bp) abolished the α1ACT fragment expression without affecting the expression of the full-length α1A subunit (Figure 1H), whereas other mutations of α1A failed to do so (Figures 1E–1H). This indicates that the 534 bp fragment upstream of the α1ACT start site in the α1A cDNA contains sequences essential for translation of α1ACT. These effects on expression were seen to an equivalent degree with both the $\alpha1A_{WT}$ and the human α1A subunit cDNA bearing the pathological polyQ tract (Q33, $\alpha1A_{SCA6}$).

CACNA1A mRNA Contains an Internal Ribosome Entry Site

We hypothesized that expression of α1ACT fragment may be mediated by an IRES present within the *CACNA1A* coding sequence. Two-dimensional structure analyses of the complete α1A mRNA sequence using an M-fold-based algorithm (Palmenberg and Sgro, 1997; Zuker, 2003) did not identify any canonical type I or type II IRES structures in this region (Baird et al., 2006). However, the region containing nucleotides 5,096–6,110 was predicted to form a highly complex, stable conformation possessing several stem-loop structures that could represent an area of functional significance for ribosomal binding and interaction with *trans*-activating factors (Figure S2). This region is highly conserved, from 89.4% in *Bos* taurus to 76.7% in *Danio* rerio (data not shown).

To test for IRES activity within this region, we inserted DNA segments of different lengths (Figure 2) from the region 5′ to the α1ACT start site into the bicistronic (Renilla luciferase, R-Luc, and firefly luciferase, F-Luc) reporter vector, pRF (Figure 2A) (Spriggs et al., 2009). Because the coding region for the R-Luc is followed by a stop codon, an increase in F-Luc activity indicates the presence of an upstream IRES that enables rebinding of the dual luciferase transcript to the ribosomal machinery. Expression of pRCT653TF or pRCT1014TF, but not pRCT189TF and pRCT293TF, in HEK293 cells enhanced the activity of the F-Luc approximately 9- and 26-fold (Figures 2A and 2B). Moreover, insertion of 1 or 2 nucleotides immediately 5′ to the ATG codon prior to the F-Luc coding region within the pRF vector eliminated the accumulation of F-Luc (Figures 2C and 2D). Therefore, the structure of the *CACNA1A* IRES is highly dependent on initiating translation of the second cistron at a specific codon, ATG 1960, as is typical of most IRES activation (Fitzgerald and Semler, 2009; Wilson et al., 2000). To help exclude the possibility that the increased F-Luc activity was due to a change at the RNA level, we inserted the same segments into the promoterless reporter vector, pGL3Basic. Transfection into HEK293 cells yielded no significant increase of luciferase activity (Figures 2E–2G), arguing against the presence of a cryptic promoter in these segments. Subsequently, we performed quantitative real-time PCR on two amplicons within the Renilla open reading frame (ORF) and one near the initiation codon of firefly ORF (Figure 2A). The observed ratio of 1:1 Renilla:Firefly mRNA (Figure 2H) favors the presence of an IRES, rather than increased transcription of the second reporter via a cryptic promoter, a splicing event or any other increase in mRNA stability. In addition, the quantitative real-time PCR expression ratios for gene fragments (5′ to or 3′ to the α1ACT start site) within the α1A subunit were approximately one in untransfected HEK293 or PC12 cells. Lastly, we found equivalent signals from before and after the α1ACT start site using endogenous α1A mRNA isolated from human cerebellum (Figures 2I and 2J). These results suggest that expression of α1ACT is driven by the presence of a cellular IRES within the α1A coding region rather than by a cryptic promoter or splicing event.

The Translocated α1ACT Fragment Binds to Noncoding Regions of Genes Expressed in Purkinje Cells and Activates Transcription

Earlier studies indicated that the 75 kDa α1ACT, bearing the normal polyQ tract, was enriched in the nucleus (Ishiguro et al., 2010; Kordasiewicz et al., 2006). To investigate whether $\alpha1ACT_{WT}$ (Q11) plays a role in gene expression by binding to genomic DNA, we performed chromatin immunoprecipitation-based cloning (ChIP-based cloning) from PC12 cells transfected with α1ACT-FLAG fusion protein (Experimental Procedures). Potential target genes identified via ChIP-based cloning and sequencing include granulin (*GRN*), B cell translation gene 1 (*BTG1*), Ca^{2+} ATPase, plasma membrane 2 (*PMCA2*), integrin α-8 precursor (*ITGA8*), and TATA box binding protein-associated factor of RNA pol II (*TAF1*) (Table S2). Putative interaction between α1ACT-FLAG fusion protein and cloned DNA segments within the *BTG1*, *PMCA2*, and *GRN* genes was further confirmed by ChIP quantitative real-time PCR (Figures 3A and 3B). Although these genes are not uniquely expressed in PCs, the

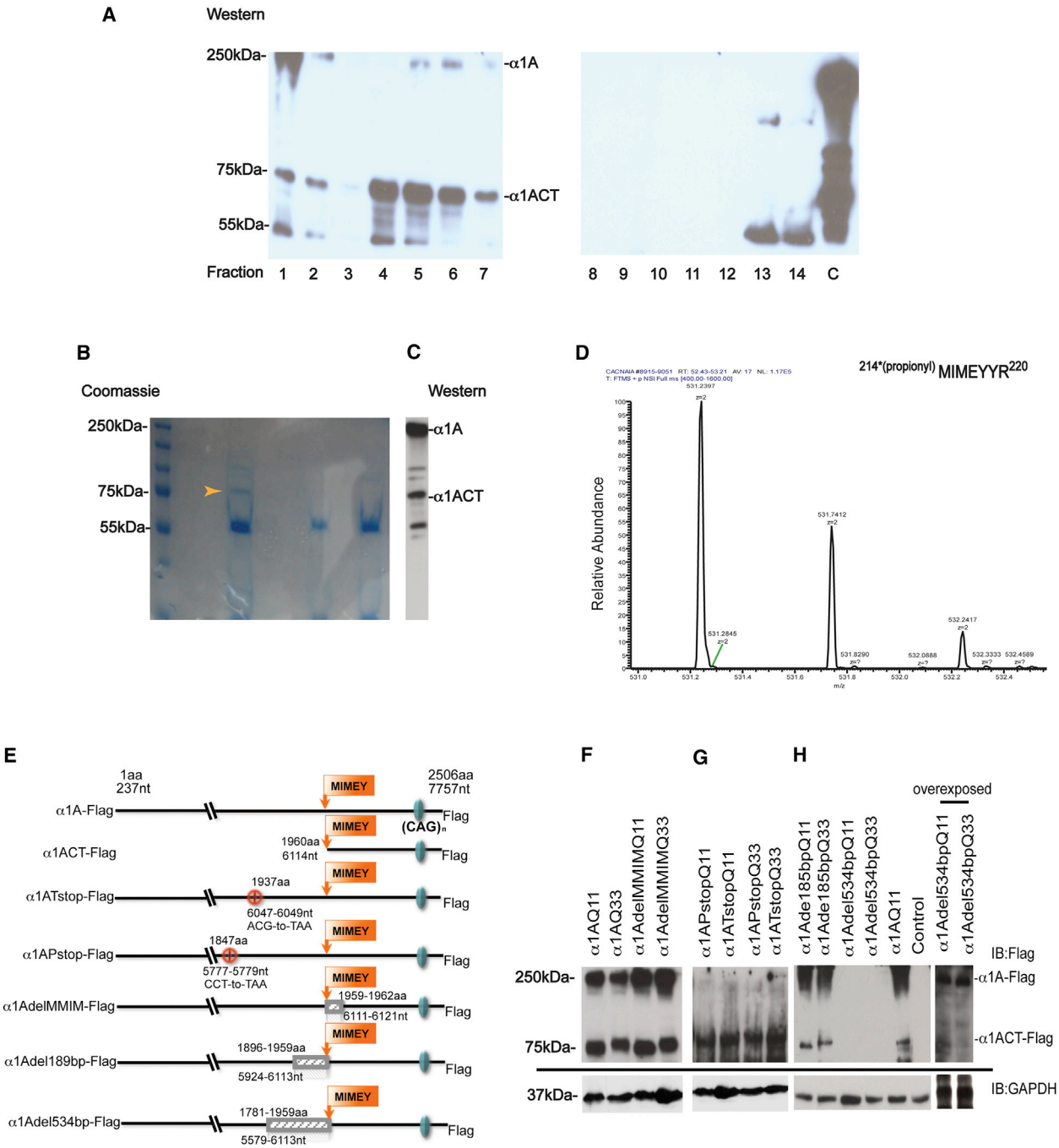

Figure 1. The C-Terminal Fragment of the α1A Subunit Initiates at MIMEY, Amino Acids 1,960–1,964, Nucleotides 6,114–6,128

(A) Western blot analysis of fractions collected from HiTrap DEAE FF anion exchange chromatography. A 3xFLAG-tagged α1A subunit is used as positive control.

(B) Coomassie blue staining of the peak α1ACT-containing fraction after two-step purification. The arrowhead indicates the 75 kDa band identified by mass spectrometry as α1ACT.

(C) Western blot analysis of lysate from α1A-overexpressing cells with anti-FLAG antibody confirms the identity of α1ACT.

(D) LC-MS/MS analysis of in-gel digest of proprionylated protein reveals that the starting amino acid sequence of N terminus of the α1ACT fragment is Met Ile Met Glu Tyr.

(E) Schematic representation of the constructs with a series of mutations or deletions.

(F) In-frame deletion of the start site of α1ACT does not abolish the expression of the 75 kDa C-terminal portion of the FLAG-tagged α1A protein bearing either normal range (Q11) or pathological range (Q33) of polyQ.

(G) Expression of the 75 kDa α1ACT C-terminal fragment persists after insertion of termination codons at T1937 or P1847 in the FLAG-tagged α1A subunit, upstream of the start site.

(legend continued on next page)

abundant expression of α1ACT in PCs suggests that they are part of a PC-specific developmental program.

We tested whether α1ACT regulates gene expression through the target sequences identified in ChIP-based cloning. Within the *BTG1* 3′ UTR, we identified an enhancer within the 113 bp sequence that was obtained from α1ACT ChIP-based cloning, using reporter assays with segments spanning three lengths (beginning at 517 nt) from the 3′ UTR inserted into the pGL3 promoter vector (Du et al., 2009), as shown in Figure 3C. Importantly, overexpression of $\alpha1ACT_{WT}$ significantly increased luciferase activity in the *BTG1*-630 reporter construct, suggesting that *BTG1* 3′ UTR contains an α1ACT-regulated enhancer element. However, $\alpha1ACT_{SCA6}$, bearing the pathological polyQ tract (Q33) failed to increase *BTG1* 3′ UTR-enhanced luciferase expression (Figure 3C). We obtained similar results from two segments of 5′ flanking region in the progranulin gene using the pGL3-basic vector. The $\alpha1ACT_{WT}$ fragment, but not the $\alpha1ACT_{SCA6}$ fragment, increased expression of the reporters bearing the 1,662 bp fragment by 2-fold and the 638 bp fragment by 3.2-fold (Figure 3D). Thus, $\alpha1ACT_{WT}$ has direct gene regulatory effects on at least two target genes, and these are lacking with $\alpha1ACT_{SCA6}$.

AT-Rich Element of α1ACT Binding Site Is Essential for the *BTG1* Enhancer Activity

Alignments of ChIP-identified sequences predict two distinct motifs, (1) an AT-rich element, TTATAAAA, and (2) a CA-rich element, CCAA, as potential α1ACT binding sites (Figure 3E). The 113 bp *BTG1* 3′ UTR sequence (517–630 bps *BTG1* wild-type [WT]; Table S3) contains both consensus sequences. As shown in Figure 3F by electrophoretic mobility shift assays (EMSA) using the *BTG1* WT as probe and nuclear extracts from untreated PC12 cells or from those transfected with $\alpha1ACT_{WT}$ and $\alpha1ACT_{SCA6}$, we observed a component in PC12 cells, caused a significant gel shift (complexes I, II, and III). This indicates that the *BTG1* 3′ UTR contains *cis*-elements reacting with neuron-specific nuclear protein, present in both untransfected and α1ACT-transfected cells. The three protein complexes with the *BTG1* WT probe could be abolished by an excess unlabeled *BTG1* WT probe, indicating that the binding was specific (lanes 3 and 4, Figure 3F). Interestingly, nuclear extracts from $\alpha1ACT_{SCA6}$-transfected PC12 cells (lane 8, Figure 3F) led to a different migration and pattern of DNA-protein complexes compared to $\alpha1ACT_{WT}$-expressing cells (lane 5, Figure 3F), with a greater abundance of complex IV in complexes from the $\alpha1ACT_{SCA6}$-transfected PC12 cells. This suggests that $\alpha1ACT_{SCA6}$ has a different protein binding pattern from $\alpha1ACT_{WT}$.

To further identify α1ACT consensus sequences, we used the AT-rich consensus element as a probe in EMSA (Table S3; Figure 3G). The AT-rich consensus sequence greatly reduced the formation of the complexes (lane 7, Figure 3G), whereas mutant AT-rich elements only partially reduced the complex formation (lanes 5 and 6, Figure 3G). Anti-FLAG antibodies generated a super-shifted complex with nuclear extracts from $\alpha1ACT_{WT}$-FLAG-expressing cells (lanes 8 and 9, Figure 3G). These studies demonstrate that α1ACT binds to an AT-rich element in the *BTG1* 3′ UTR. Finally, we performed EMSA with a series of 3 bp mutations of the TTATAAGAT sequence (Table S3). As shown in Figure 3H, Mut1 abolished complex II and Mut2 abolished complex I. Mut4, combining Mut1 and Mut2, abolished both complexes I and II (Figure S3). We also mutated the element, TTATAAGT, within the *BTG1*-630 reporter construct (517–630 bp). Constructs 630mut1 and 630mut2 contain 3 bp mutation, whereas 630mut4 contains both Mut1 and Mut2 substitutions. All three constructs had significantly reduced luciferase activities, both basally and in response to overexpressing of $\alpha1ACT_{WT}$ compared to *BTG1* 630 construct (Figure 3I). These results suggest that TTATAA is the core sequence of the AT-rich element that is required to maintain the α1ACT-regulated *BTG1* expression.

The $\alpha1ACT_{WT}$, but Not $\alpha1ACT_{SCA6}$, Increases the Physiological Expression of Target Genes and Enhances Neurite Outgrowth of Differentiating PC12 Cells

To test for an effect of α1ACT on endogenous expression of ChIP-identified genes, we examined the mRNA and protein levels of *TAF*, *BTG1*, *PMCA2*, and *GRN* in both cell lines and human cerebellum. Overexpression of normal $\alpha1A_{WT}$ or $\alpha1ACT_{WT}$, but not $\alpha1ACT_{SCA6}$, significantly increased the expression of these genes (1.6- to 2.7-fold) in PC12 cells, either compared to empty vector-transfected or $\alpha1ACT_{SCA6}$-transfected PC12 cells (Figure 4A). As shown in Figures 4B and 4C, BTG1 and PMCA2 protein expression levels were also increased in $\alpha1A_{WT}$- and $\alpha1ACT_{WT}$-transfected PC12 cells. Finally, using cerebellar tissues from two SCA6 patients (Q22) and normalizing transcript levels to a PC-specific mRNA, Pcp2, we found that *BTG1* gene mRNA expression was decreased compared to the normal control (Figure 4D).

Several of the genes regulated by α1ACT are known to play a role in differentiation of the neuronal phenotype (Baker et al., 2006). We established PC12 cell lines stably expressing 3xFLAG-tagged versions of either the full-length α1A or the α1ACT fragment. Upon induction with nerve growth factor (NGF) for 24 hr, we observed that both $\alpha1A_{WT}$-FLAG and $\alpha1ACT_{WT}$-FLAG enhanced neurite outgrowth (fraction of cells with neurites) when compared with PC12 cells expressing empty vector (Figures 4E–4H; Figures S4A–S4D). Importantly, the P/Q channel blocker, ω-agatoxin, had no effect on $\alpha1ACT_{WT}$-induced neurite outgrowth (Figure S4E). Furthermore, blocking the expression of endogenous or transfected full-length α1A by small interference RNA (siRNA) had no effect on $\alpha1ACT_{WT}$-enhanced neurite outgrowth in PC12 cells transfected with $\alpha1ACT_{WT}$-FLAG (Figures S4E–S4K). These findings suggest that enhanced neurite outgrowth does not depend on functioning channels or the presence of the full channel protein.

(H) Deletion of a 534 bp fragment (α1Adel534Q11), but not deletion of a 185 bp fragment (α1Adel185Q11), from the α1A coding region upstream of the α1ACT eliminates α1ACT expression, while maintaining expression of full-length α1A-FLAG. Deletions using encoded Q33 repeat expansions constructs (α1Adel185Q33 and α1Adel534Q33) behave similar to the Q11 constructs.
See also Figure S1.

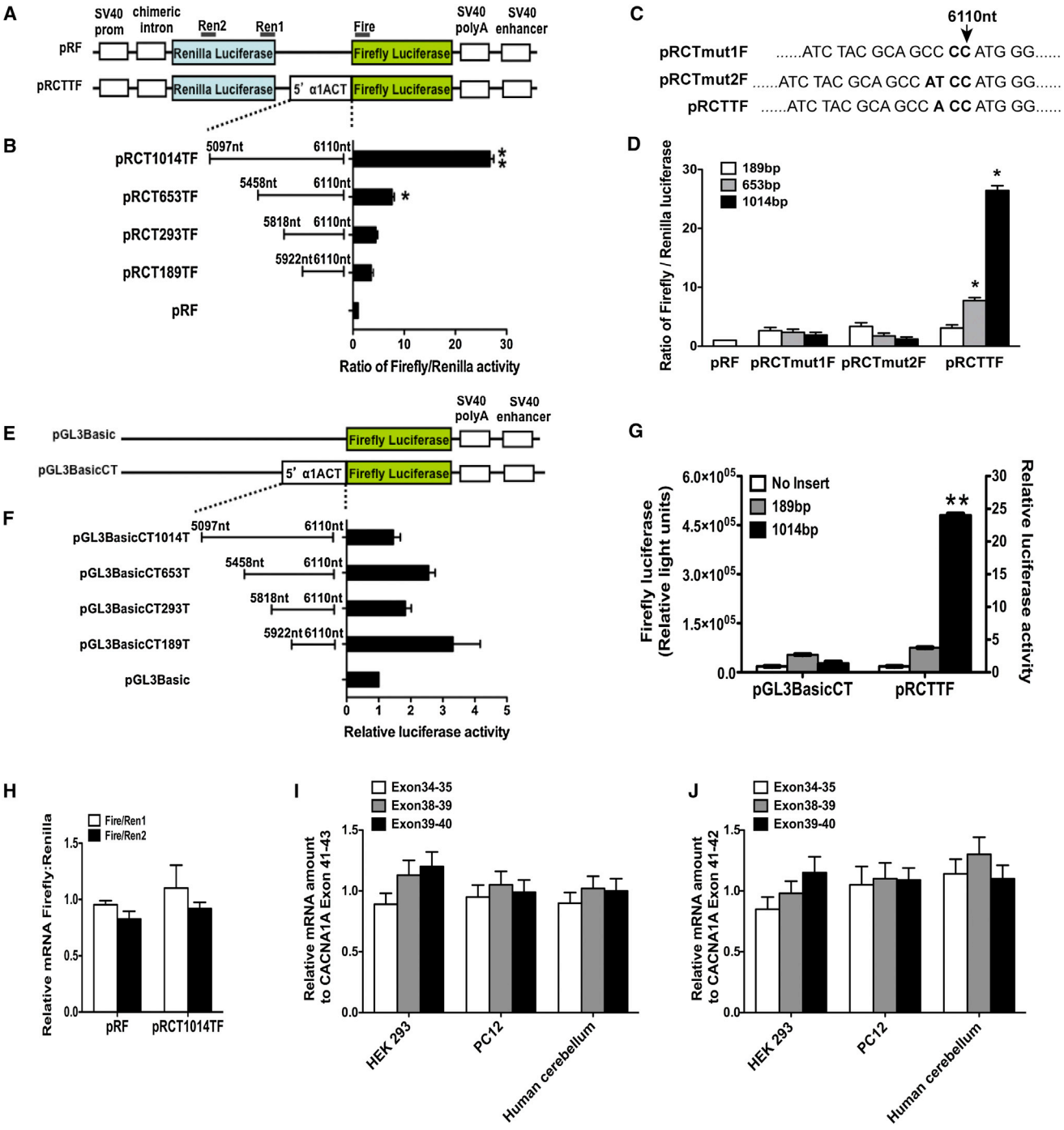

Figure 2. *CACNA1A* mRNA Contains an IRES

(A) Schematic representation of the constructs pRF and pRCTTF.

(B) IRES activity is demonstrated using bicistronic vectors. The ratio of Renilla luciferase and firefly luciferase activities was determined and normalized to β-galactosidase activities.

(C) Sequence of *CACNA1A* IRES nucleotide inserts CTT, CTmut1, and CTmut2, inserting of 1 to 2 nucleotides.

(D) The luciferase activities of bicistronic vectors bearing nucleotide insertions are determined as in (B).

(E) Schematic representation of the constructs pGL3Basic and pGL3BasicCT. The same DNA fragments as inserted into pRF were subcloned into the promoterless pGL3Basic construct.

(F) Luciferase activities are determined as in (B).

(G) The raw firefly luciferase activities of two fragments are compared between promoterless vector pGL3BasicCT and bicistronic vector pRCTTF, which suggests that the 1,014 bp fragment contains an IRES.

(legend continued on next page)

There was a significant increase in the percentage of cells bearing neurites in cells transfected with $\alpha1A_{WT}$-FLAG and $\alpha1ACT_{WT}$-FLAG compared to controls after NGF stimulation for 24, 48, and 72 hr (Figures 4E, 4F, and 4H). Total neurite lengths were also increased 2-fold in $\alpha1ACT_{WT}$-expressing cells compared with controls at each time point (Figure 4G; Figures S4A–S4D). However, cells expressing $\alpha1ACT_{SCA6}$-FLAG had significantly lower percentage of cells with neurites and total neurite length/cell compared with cells expressing $\alpha1ACT_{WT}$-FLAG (Figures 4E–4H; Figures S4A–S4D). Thus, $\alpha1ACT_{SCA6}$ lacks the normal function of $\alpha1ACT_{WT}$ in potentiating neurite outgrowth in neuronal cells.

BTG1 belongs to the BTG/TOB protein family of antiproliferative genes. Both BTG1 and BTG2 proteins interact with the protein arginine N-methyltransferase (i.e., PRMT1) and positively modulate its activity. The PRMT1/BTG methylation pathway is involved in maintaining neuronal cells in a differentiated state (Berthet et al., 2002). We used BTG1 antibody to immunoprecipitate PRMT1 in PC12 cells stably transfected with $\alpha1ACT_{WT}$ and $\alpha1ACT_{SCA6}$. In $\alpha1ACT_{WT}$-expressing cells, the quantity of precipitated PRMT1 was increased, whereas in $\alpha1ACT_{SCA6}$-expressing cells, precipitated PRMT1 was decreased, consistent with the expression of BTG1 in these two cell types (Figure 4I). Meanwhile, silencing of BTG1 by siRNA blocked the NGF-induced α1ACT-regulated neurite outgrowth (Figures 4J–4L; Figure S4L). These results demonstrate that α1ACT with normal range polyQ maintains the physiological expression of the *BTG1* gene, leading to subsequent interaction of the PRMT1/BTG pathway to mediate neuronal differentiation. Together, these observations suggest that the normal α1ACT acts as a transcription factor through target genes to enhance the neuronal phenotype and that one effect of the SCA6 polyQ expansion in α1ACT is to disrupt the properties of the α1ACT transcription factor.

α1ACT Partially Rescues the Phenotype of $\alpha1A^{-/-}$ Mice

$\alpha1A^{-/-}$ mice, with targeted disruption of mouse *CACNA1A*, develop a gross neurological phenotype of seizures, dystonia, and ataxia soon after birth and die by P18–P21 (Jun et al., 1999). To investigate the importance of expression of the α1ACT fragment in PCs, we used the Pcp2 promoter and Tet-off system (Zu et al., 2004) to generate two double transgenic mouse lines, Pcp2-tTA/TRE-α1ACT (abbreviated, PC-α1ACT), expressing at comparable levels either $\alpha1ACT_{WT}$ (WT = Q4, the smallest α1ACT polyQ seen in humans) or $\alpha1ACT_{SCA6}$ (SCA6 = Q33, the largest α1ACT polyQ seen in SCA6) fragments tagged with an N-terminal myc epitope (see Experimental Procedures). These mice appeared to grow and develop normally and live a full lifespan. $\alpha1ACT_{SCA6}$ mice, however, had mild progressive motor problems that were evident using the treadmill (see below).

To test the role of α1ACT in cerebellar PC development in the absence of α1A channels, we bred PC-α1ACT mice with $\alpha1A^{+/-}$ heterozygous knockout mice and subsequently crossed these offspring to generate $\alpha1A^{-/-}$ mice with PC-targeted α1ACT expression ($\alpha1A^{-/-}$/PC-α1ACT). Curiously, we did not identify any mice with $\alpha1A^{-/-}$/PC-$\alpha1ACT_{SCA6}$ genotype, suggesting an impaired viability (Figure 5A). As expected, $\alpha1A^{-/-}$ exhibited severe neurological impairment (Jun et al., 1999). Surprisingly, $\alpha1A^{-/-}$ mice expressing $\alpha1ACT_{WT}$, i.e., $\alpha1A^{-/-}$/PC-$\alpha1ACT_{WT}$ mice, had an improved behavioral phenotype relative to $\alpha1A^{-/-}$ mice. Although still neurologically impaired, they gained more weight during the first 2 weeks of postnatal life compared to $\alpha1A^{-/-}$ mice (Figures 5B and 5C), had improved in-cage mobility (Movie S1), and survived ~1 week longer than $\alpha1A^{-/-}$ mice (Figure 5D). We reasoned that the improved phenotype of $\alpha1A^{-/-}$/PC-$\alpha1ACT_{WT}$ mouse might be mediated through improved dendritic and synaptic development. Immunofluorescent staining of cerebellar cortex of P16 mice from three groups, WT, $\alpha1A^{-/-}$, and $\alpha1A^{-/-}$/PC-$\alpha1ACT_{WT}$ mice showed that, as noted previously, PCs of $\alpha1A^{-/-}$ mice had shortened primary dendrites with premature branching and an immature pattern of parallel fiber (PF) and climbing fiber (CF) synaptic contacts on PC soma and proximal dendrites (Hashimoto et al., 2011) (Figures 5E–5L). In contrast, PC morphology and afferent innervation of $\alpha1A^{-/-}$/PC-$\alpha1ACT_{WT}$ cells resembled the pattern in WT mice (Figures 5E–5L). In $\alpha1A^{-/-}$/PC-$\alpha1ACT_{WT}$ mice, the thickness of molecular layer (ML), the relative height, and density of the dendritic tree were significantly increased, compared to those of $\alpha1A^{-/-}$ mice ($p < 0.05$) (Figures 5F–5H). This finding is consistent with our in vitro studies showing that α1ACT enhances neurite outgrowth.

We also compared the height of CF innervation between the three mouse groups (Figures 5J–5L) (Hashimoto and Kano, 2005; Hashimoto et al., 2011). In $\alpha1A^{-/-}$ mice, most PCs were multi-innervated, and the CF height only reached 65.2% ± 5.3% of the ML at P16. We found that the CF height was improved in $\alpha1A^{-/-}$/PC-$\alpha1ACT_{WT}$ mice over that of $\alpha1A^{-/-}$ mice, reaching to 80.7% ± 4.1% of the ML at P16 ($p < 0.05$). However, $\alpha1A^{-/-}$/PC-$\alpha1ACT_{WT}$ mice exhibited the same three patterns of CF contacts seen with $\alpha1A^{-/-}$ mice, mono CF on PC dendrites, multiple CF contacts on proximal dendrites, and multiple CF contacts on PC soma (Figure 5). These results demonstrate that α1ACT, as a transcription factor, plays an important role in establishing normal dendritic tree morphology in PCs in vivo but that synapse elimination or selection of dominant innervation requires either P/Q channel function or α1ACT under its endogenous expression pattern.

Finally, we examined mRNA levels of *TAF*, *BTG1*, *PMCA2*, and *GRN* in the three mouse groups. Figure S5 demonstrates that the expression of these genes was decreased in cerebellar tissue of $\alpha1A^{-/-}$ mice when compared to normal mice but was increased 1.5- to 3-fold in $\alpha1A^{-/-}$/PC-$\alpha1ACT_{WT}$ transgenic mice when compared to $\alpha1A^{-/-}$ mice ($p < 0.05$), relative to either β-actin

(H) Quantitative real-time PCR performed using RNA from cells transfected with bicistronic vectors as amplified using primers Ren1, Ren2, and Fire demonstrates no difference in abundance of R-Luc and F-Luc mRNA.

(I and J) Quantitative real-time PCR performed using RNA extracted from PC12 and HEK293 cells, transfected with α1A or human cerebellum to compare abundance of amplicons Ex34–35, Ex38–39, and Ex39–40 upstream of the α1ACT start site relative to amplicons Ex41–42 (I) and Ex41–43 (J), from within the α1ACT coding region. Data are mean ± SEM, $n \geq 3$ (each involving triplicate assays, *$p < 0.05$, **$p < 0.01$).

See also Figure S2.

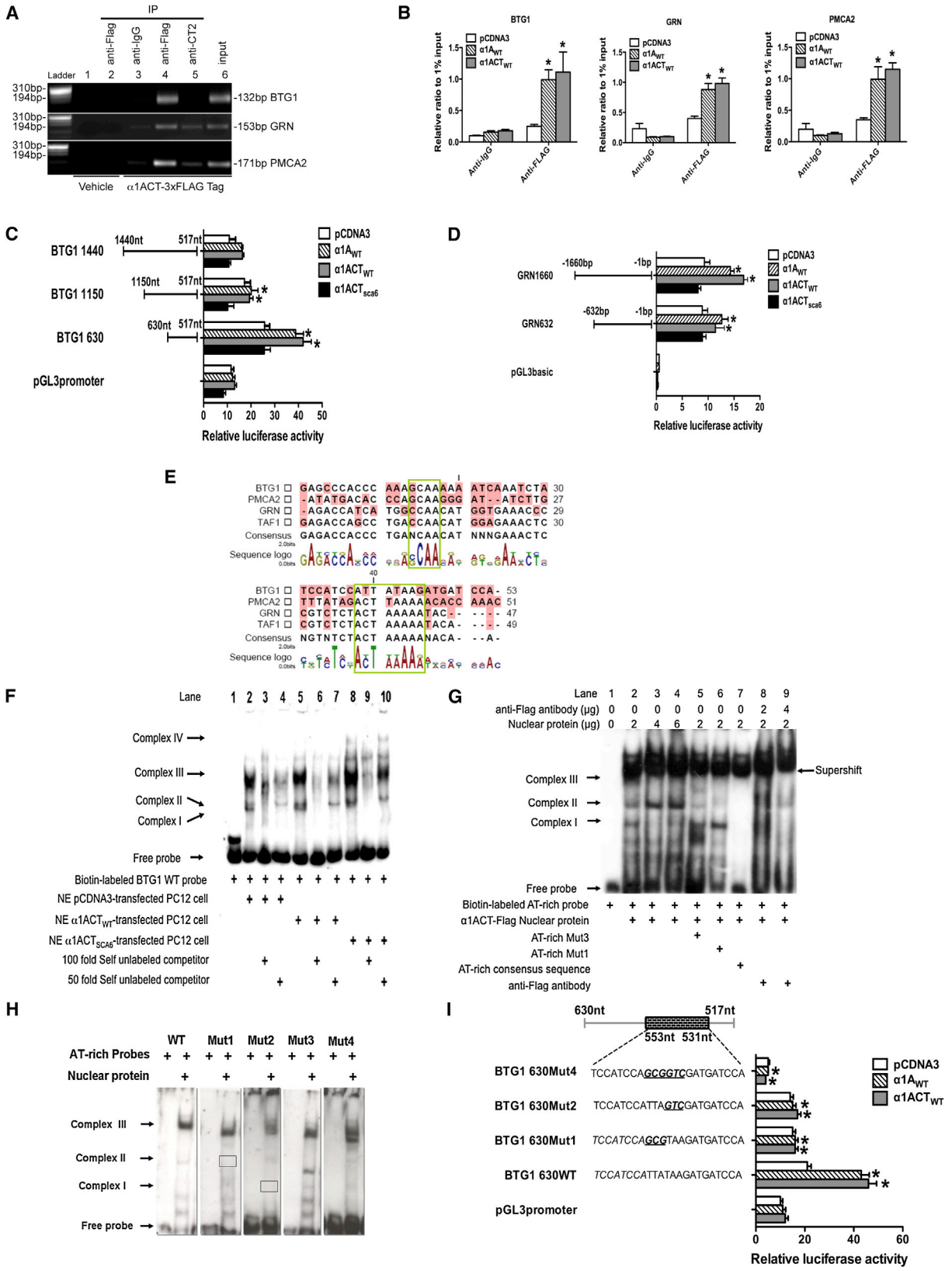

(legend on next page)

or Pcp2 gene expression (Figures S5A–S5D). These results indicate that expression of the α1ACT target genes is impaired in $\alpha 1A^{-/-}$ mice and is corrected by localized expression of $\alpha 1ACT_{WT}$ in PCs of transgenic mice.

α1ACT Partially Restores Parallel Fiber EPSC Amplitude, but Not Climbing Fiber Monoinnervation

To further assess the effect of α1ACT expression on Purkinje cell synaptic properties, we measured PF excitatory postsynaptic current (PF-EPSC) amplitude as a function of stimulus intensity in WT, $\alpha 1A^{-/-}$, and $\alpha 1A^{-/-}$/PC-$\alpha 1ACT_{WT}$ mice (P16–P18) in cerebellar slice preparations. Whereas PF-EPSCs from WT were significantly larger than those from both $\alpha 1A^{-/-}$ mice ($p < 0.01$, stimulus intensities 20–55 μA) and $\alpha 1A^{-/-}$/PC-$\alpha 1ACT_{WT}$ mice ($p < 0.05$), EPSCs from $\alpha 1A^{-/-}$/PC-$\alpha 1ACT_{WT}$ mice were greater than those from $\alpha 1A^{-/-}$ mice ($p < 0.05$), indicating that α1ACT expression improves PF synaptic connections (Figure 6A).

The inability of α1ACT to completely restore EPSC amplitudes to WT levels could be explained by the absence of P/Q-type Ca^{2+} channels in PF presynaptic terminals of $\alpha 1A^{-/-}$/PC-$\alpha 1ACT_{WT}$ mice, as these channels play a critical role in neurotransmitter release at PF-Purkinje cell (PF-PC) synapses (Matsushita et al., 2002; Mintz et al., 1995). We therefore examined the presynaptic release properties of PF-PC synapses in $\alpha 1A^{-/-}$ and $\alpha 1A^{-/-}$/PC-$\alpha 1ACT_{WT}$ mice by measuring the paired-pulse ratios (PPRs) of PF-EPSCs. Large PPRs are indicative of low initial release probabilities and are a sign of impaired presynaptic function (Zucker and Regehr, 2002). In accordance with observations from mouse models harboring loss-of-function mutations in the *CACNA1A* gene, $\alpha 1A^{-/-}$ mice exhibited PPRs significantly greater than WT at several stimulus intervals (WT to $\alpha 1A^{-/-}$ mice: $p < 0.01$ for stimulus intervals of 20–100 ms, Figure 6B) (Liu and Friel, 2008; Matsushita et al., 2002). Whereas α1ACT expression did lower PPRs closer to WT levels ($\alpha 1A^{-/-}$/PC-$\alpha 1ACT_{WT}$ to $\alpha 1A^{-/-}$ mice: $p < 0.01$ for stimulus intervals of 20 and 100 ms, $p < 0.05$ for stimulus interval of 50 ms), the measured values were still elevated (WT to $\alpha 1A^{-/-}$/PC-$\alpha 1ACT_{WT}$: $p < 0.05$ for stimulus intervals of 20 and 50 ms) (Figure 6B), suggesting a residual presynaptic deficit.

We also examined properties of the CF synapse onto Purkinje cells. We observed a reduction in CF EPSC amplitudes and a decrease in the degree of paired-pulse depression in both $\alpha 1A^{-/-}$ and $\alpha 1A^{-/-}$/PC-$\alpha 1ACT_{WT}$ mice with respect to WT, both of which could also be due to the absence of P/Q-type channels presynaptically (Figure 6C). Additionally, we investigated whether α1ACT expression affects the process of CF maturation. During development, Purkinje cells undergo a competitive and activity-dependent elimination of superfluous CF inputs until only one remains. Impairments to this process result in the persistent innervation of Purkinje cells by multiple climbing fibers into adulthood. We found the proportion of Purkinje cells with multiple CF innervations to be increased in both $\alpha 1A^{-/-}$ and $\alpha 1A^{-/-}$/PC-$\alpha 1ACT_{WT}$ mice compared to WT, a result indicating that actual P/Q-type Ca^{2+} channel function, and not just expression of the C terminus, may be essential for proper CF maturation (Watanabe and Kano, 2011) (Figure 6D). Our results provide evidence that α1ACT expression improves the synaptic connections of PFs, but not CFs, onto Purkinje cells.

$\alpha 1ACT_{SCA6}$ Causes Cell Death In Vitro and Mediates Ataxia and Cerebellar Cortical Atrophy in Transgenic Mice

Previous studies have shown that the α1A C terminus bearing an expanded polyQ tract is toxic relative to WT α1A C terminus when transiently overexpressed in cultured mammalian cells (Ishiguro et al., 2010; Kubodera et al., 2003). Our flow cytometry results showed that PC12 cells stably expressing $\alpha 1ACT_{WT}$ exhibited equivalent viability to vector control cells, whereas cells expressing $\alpha 1ACT_{SCA6}$ had an ~2-fold increase in cell death ($p < 0.05$, Figure 7A–7C) (Koopman et al., 1994). Also, lactate dehydrogenase (LDH) release was significantly higher in cells expressing the $\alpha 1ACT_{SCA6}$ compared with that of PC12 cells expressing only pcDNA3 or $\alpha 1ACT_{WT}$ (Figure 7D). These findings indicate that overexpression of α1ACT bearing pathological size of polyQ reduces cell viability in cultured mammalian cells.

Finally, we tested whether overexpression of the SCA6-expanded $\alpha 1ACT_{SCA6}$ fragment in mice would lead to clinical or pathological features resembling SCA6, compared with

Figure 3. α1ACT Is a Transcription Factor that Regulates Neural Gene Expression through an AT-Rich Element

(A) ChIP and quantitative real-time PCR verification of DNA sequences identified by ChIP cloning. PC12 cells were transfected with empty vector or FLAG-tagged $\alpha 1ACT_{WT}$.

(B) Relative enrichment was calculated as the ratio between the net intensity of each bound sample normalized to its input sample and the vehicle control sample normalized to vehicle control input sample ($n \geq 3$).

(C) Enhancer activity of *BTG1* gene fragments. Positions of the fragments are indicated.

(D) Promoter activity of *GRN* gene fragments. Positions of the fragments are indicated.

(E) Consensus sequence analyzed by CLC main workbench (v. 6.5) among the α1ACT ChIP-targeted sequences. Consensus sequence was predicted and labeled in red.

(F) EMSA demonstrates the formation of displaceable nucleoprotein complex with the α1ACT and *BTG1* WT (517–630 nt) element. Lane 1 is biotin-labeled *BTG1* WT probe. Lanes 2 and 5 show the three major complexes formed between BTG1 probe and $\alpha 1ACT_{WT}$ nuclear protein. Lane 8 shows the fourth complex formed between BTG1 probe and $\alpha 1ACT_{SCA6}$ nuclear protein.

(G) EMSA shows that the AT-rich probe (531–553 nt) forms three complexes in the absence of competitor. These complexes were displaced by excess unlabeled AT-rich sequence and partially abolished by AT-rich Mut1 and Mut3. The super-shifted bands were only seen in $\alpha 1ACT_{WT}$-FLAG nuclear extracts treated with FLAG-M2 antibodies, but not in lane of pCDNA3 nuclear extracts.

(H) EMSA shows that the TTATAA region is critical for the formation of nucleoprotein complexes with AT-rich element.

(I) $\alpha 1ACT_{WT}$ significantly increases BTG1 enhancer activity through intact TTATAA region. Plasmid pRL-TK is used as transfection efficiency control. Data are mean ± SEM, $n \geq 3$ (each involving triplicate assays, $^*p < 0.05$ versus control construct).

See also Figure S3.

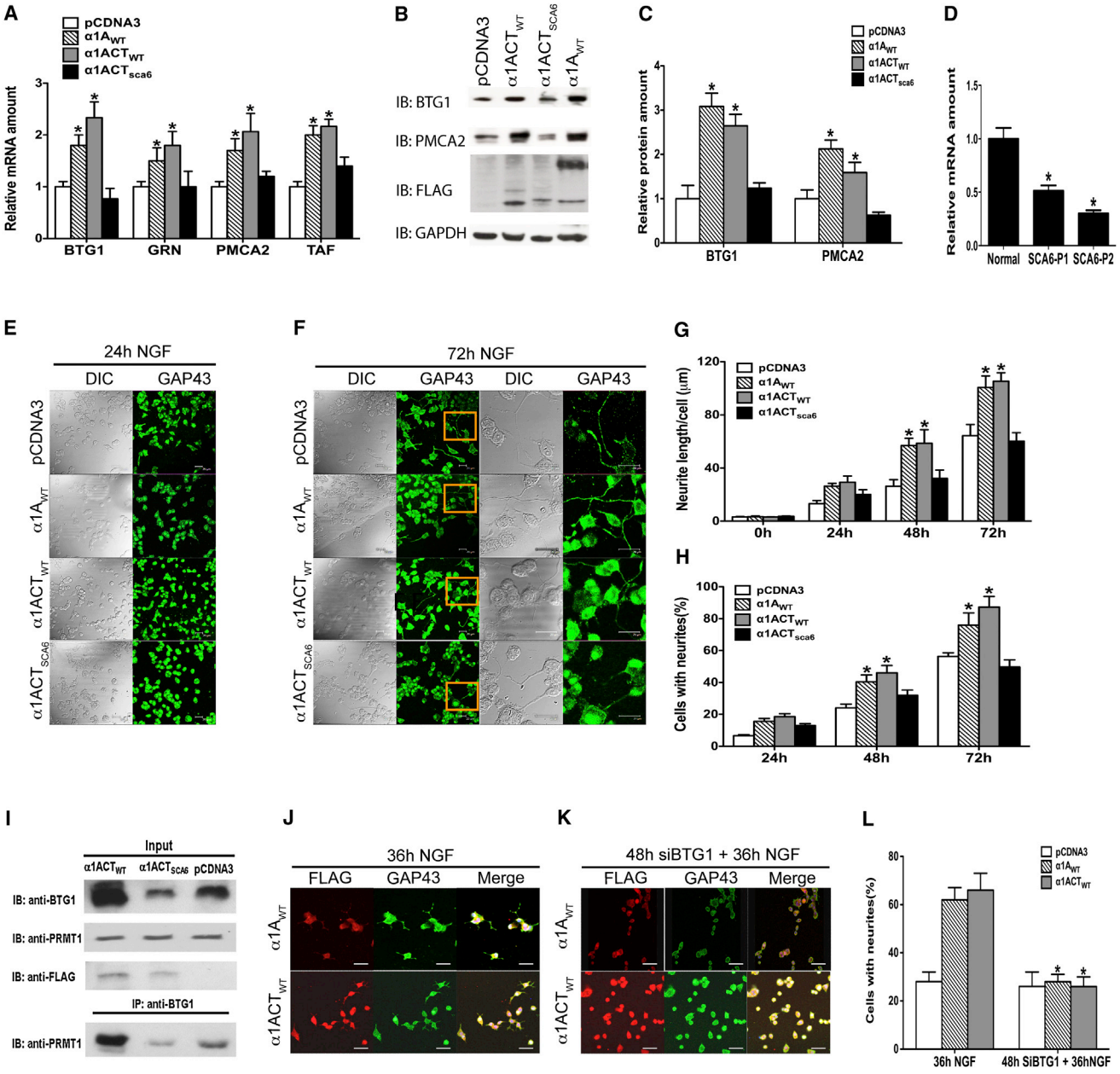

Figure 4. α1ACT Enhances Neurite Outgrowth by Regulating *BTG1* Expression

(A) Relative mRNA expression levels of *BTG1*, *PMCA2*, *TAF*, and *GRN* in PC12 cells transfected with $\alpha1A_{WT}$, $\alpha1ACT_{WT}$, or $\alpha1ACT_{SCA6}$ ($n \geq 3$).

(B and C) Western blot (B) and quantitation of protein expression levels of BTG1 and PMCA2 in PC12 cells transfected with $\alpha1A_{WT}$, $\alpha1ACT_{WT}$, and $\alpha1ACT_{SCA6}$ (C).

(D) Relative levels of *BTG1* mRNA in the cerebellum from two SCA6 patients, normalized to Pcp2.

(E and F) $\alpha1ACT_{WT}$ enhances neurite outgrowth. Representative low- and high-magnification images of PC12 cells with transiently transfected pcDNA3-FLAG, $\alpha1A_{WT}$-FLAG, $\alpha1ACT_{WT}$-FLAG, and $\alpha1ACT_{SCA6}$-FLAG at 24 hr (E) and 72 hr after NGF treatment (F). Cells were labeled for GAP-43 (green) to visualize PC12 cell body and neurites.

(G and H) Quantitation of average neurite length and percentage of neurites per cell (n = 200; *$p < 0.05$ versus pcDNA3-FLAG).

(I) $\alpha1ACT_{WT}$ upregulates *BTG1* gene and increases PRMT1/BTG1 protein interaction.

(J and K) Silencing of *BTG1* expression inhibits $\alpha1ACT_{WT}$-enhanced neurite outgrowth. Anti-FLAG staining is shown in red.

(L) Quantitation of neurite outgrowth by siBTG1 in transfected cells (n = 3, *$p < 0.05$). The blunted effect by $\alpha1ACT_{SCA6}$-FLAG was also diminished by BTG1 silencing. Data are mean ± SEM.

See also Figure S4.

overexpression of the fragment with normal allele size, $\alpha 1ACT_{WT}$. Both $\alpha 1ACT_{WT}$ and $\alpha 1ACT_{SCA6}$ can be detected in the nucleus of PCs in the corresponding PC-α1ACT lines at comparable levels by western blot, quantitative real-time PCR, and immunostaining (Figure 7E; Figures S6A and S6B). There were no obvious clinical differences between these two lines in young adults, and lifespan was not affected. However, we found that PC-$\alpha 1ACT_{SCA6}$ mice demonstrated significant abnormalities in several gait parameters compared with PC-$\alpha 1ACT_{WT}$ mice using a video-assisted computerized treadmill for gait analysis (DigiGait, Mouse Specifics) ($p < 0.05$, after post hoc correction). Most importantly, they exhibited an age-dependent increase in shared stance (double support time) of hind limbs, between 3 and 9 months old, indicating progressive instability during walking ($p < 0.05$, Figure 7F; Movies S2 and S3) (Matsukawa et al., 2003; Stolze et al., 2002). The gait disturbance never progressed to the level of severe ataxia, although natural changes in weight gain in older mice may have obscured an impact on normal cage activity. The lack of severe ataxia even in 2-year-old mice is not surprising for a model of SCA6, with an age of onset of 43–52 years. Although we found no obvious sign of cell loss in the cerebellum in $\alpha 1ACT_{SCA6}$ mice at ~2 years of age, measurement of the ML thickness showed that $\alpha 1ACT_{SCA6}$-expressing mice have significant thinning of the ML, compared with age-matched $\alpha 1ACT_{WT}$ and WT mice (Figures 7G and 7H). Lastly, using quantitative real-time PCR to examine the expression levels of ChIP-identified genes *TAF*, *GRN*, *BTG1*, and *PMCA2* in cerebellar tissues of 2-year-old PC-$\alpha 1ACT_{SCA6}$ mice compared with age-matched WT mice, we found that the transcript levels of each of the α1ACT-regulated genes were decreased by between 11% and 34% (Figures S6C–S6F). These findings are the first to demonstrate clinical and pathological changes in an animal model of SCA6 expressing appropriate-sized pathological alleles within a *CACNA1A*-encoded protein.

DISCUSSION

CACNA1A Contains a Cellular IRES

Cellular IRESs play an increasingly recognized role in the control of eukaryote gene expression, where in many 5′ UTRs they provide alternatives to cap-dependent translation initiation during times of cellular stress (Coldwell et al., 2001; Spriggs et al., 2008). IRES sequences have also been detected within the coding regions of some cellular mRNAs, leading to the expression of isoforms or distinct protein products (Cornelis et al., 2000; Ul-Hussain et al., 2008). Together with the present report, these observations suggest that expression of bifunctional genes, particularly those encoding separate transcription factor proteins in the second cistron, may be a strategy for coordinating gene expression programs tied to individual gene products. This could enable the timely expression of a set of genes coincident with the appearance of key proteins during differentiation.

α1ACT, a *CACNA1A*-Encoded Transcription Factor, Promotes a Neurite Outgrowth Program

As a transcription factor, the normal α1ACT enhances the expression of at least three genes, *GRN*, *PMCA2*, and *BTG1*, in PC12 cells and cerebellar tissue, potentiates NGF-mediated neurite outgrowth in PC12 cells, and partially rescues the *CACNA1A* knockout phenotype. GRN is involved in neurite outgrowth and is critical in maintaining neuronal survival because loss-of-function mutations of the *GRN* gene lead to cell death in the frontal and temporal lobes (Baker et al., 2006; Cruts et al., 2006; Van Damme et al., 2008). *PMCA2* is highly expressed in the cerebellum, particularly in PCs and throughout the ML and granule cell layer (Zacharias and Kappen, 1999). PMCA2 knockout mice exhibit vestibular and gait abnormalities and reduced thickness of the cerebellar ML (Kozel et al., 1998). Lack of PMCA2 also dramatically alters PC morphology. PMCA2 is a component of mGluR1-IP3R1 signaling complex, which has been implicated in plasticity at the PF-PC synapse (Kurnellas et al., 2007).

The PRMT1/BTG methylation pathway is involved in neurogenesis or in maintaining neuronal cells in a differentiated state. The 3′ UTR of BTG1 is highly conserved throughout evolution and plays a key role in this pathway (Rouault et al., 1993), consistent with our finding that α1ACT activates a novel 3′ enhancer element of BTG1. Enhanced BTG1/PRMT1-driven arginine methylation partly accounts for the essential role of protein methylation during PC12 differentiation (Cimato et al., 1997), which is in line with findings here that BTG1 knockdown blocks neurite outgrowth. Together, these findings suggest that $\alpha 1ACT_{WT}$ is essential for maintenance of neurite outgrowth through gene-specific signaling pathways. It will be of interest to extend our ChIP-based cloning approach using RNA-seq methodology to more completely characterize the normal repertoire of α1ACT-regulated genes, as well as those bound by $\alpha 1ACT_{SCA6}$.

Except for the in vivo studies, the properties of α1ACT are similar to those demonstrated for the 70 kDa fragment, termed CCAT, derived from the Cav1.2 channel, α1C subunit, which may arise from a similar translational mechanism (Gomez-Ospina et al., 2006). In that case, as well as in ours, the set of genes regulated by these transcription factors does not conform to an obvious functional class of proteins but appears to be involved in elaborating key components of the neuronal phenotype and in neurogenesis or neurodegeneration, timed with the appearance of Ca^{2+} channel activity.

Phenotype Rescue of $\alpha 1A^{-/-}$ Mice by α1ACT

The improved phenotype at behavioral, histological, and electrophysiological levels in $\alpha 1A^{-/-}$/PC-$\alpha 1ACT_{WT}$ mice is remarkable, particularly because $\alpha 1ACT_{WT}$ expression, under the control of PC specific promoter, Pcp2, was only restored in PCs. Consistent with these findings and our in vitro results, ChIP-identified genes *TAF*, *BTG1*, *PMCA2*, and *GRN* were downregulated in $\alpha 1A^{-/-}$ mice but were increased 1.5- to 3-fold in $\alpha 1A^{-/-}$/PC-$\alpha 1ACT_{WT}$ transgenic mice. These results suggest that α1ACT, as a second gene product from *CACNA1A*, plays an important role in establishing normal morphology and function of PCs.

α1ACT Expression Improves PF-PC Connections

PF-EPSC amplitudes measured in $\alpha 1A^{-/-}$/PC-$\alpha 1ACT_{WT}$ were significantly greater than those observed in $\alpha 1A^{-/-}$ mice, though they were not completely restored to WT levels, presumably due

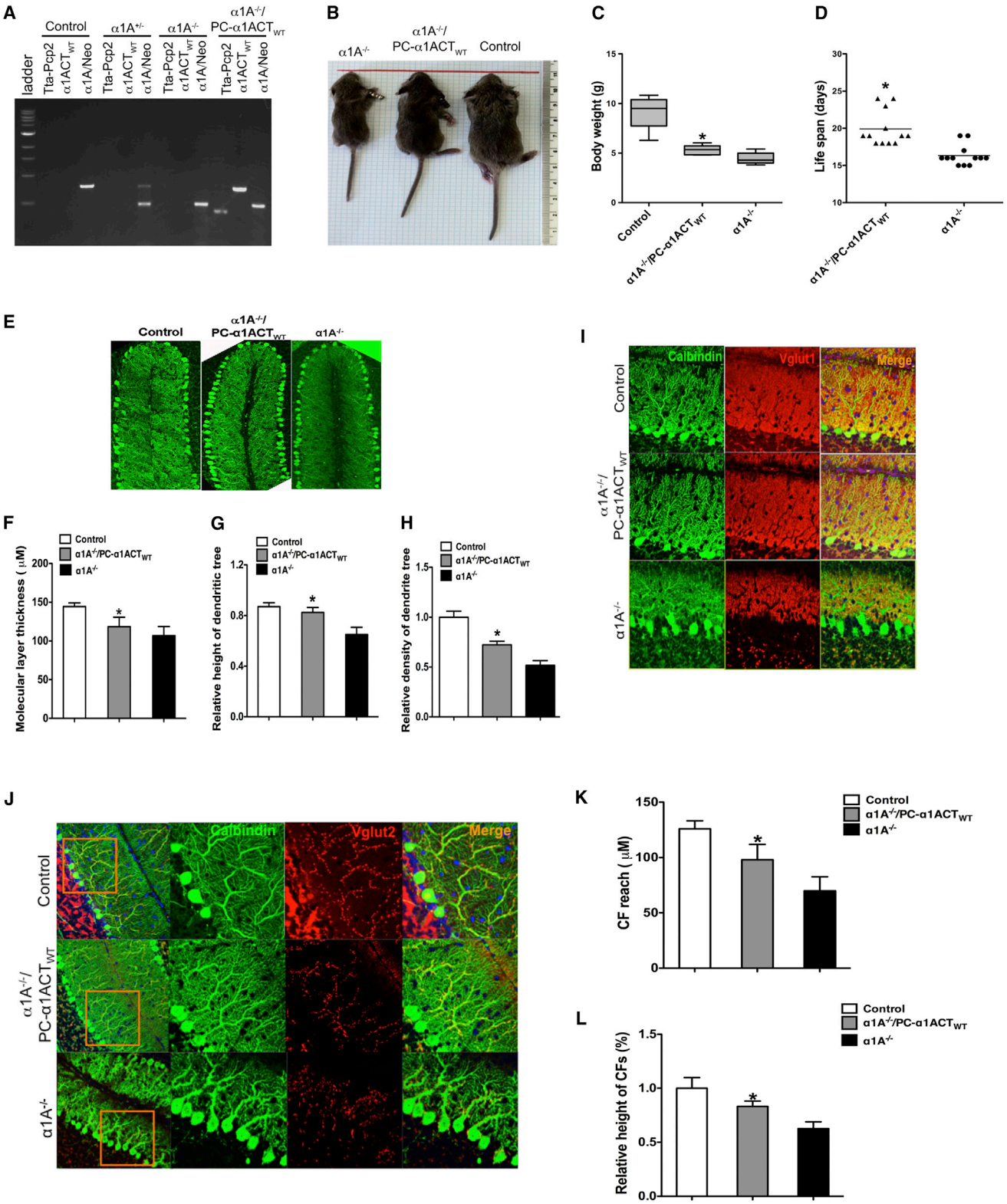

Figure 5. $\alpha 1A^{-/-}$/PC-α1ACT$_{WT}$ Transgenic Mice Have Improved Phenotype and Development of Cerebellar Cortex, as Compared to $\alpha 1A^{-/-}$ Mice

(A and B) The genotype (A) and appearance (B) of $\alpha 1A^{-/-}$/PC-α1ACT$_{WT}$ mice.

(C) $\alpha 1A^{-/-}$/PC-α1ACT$_{WT}$ mice had slightly greater body weight compared with $\alpha 1A^{-/-}$ mice at age of P14 (*$p < 0.05$).

(legend continued on next page)

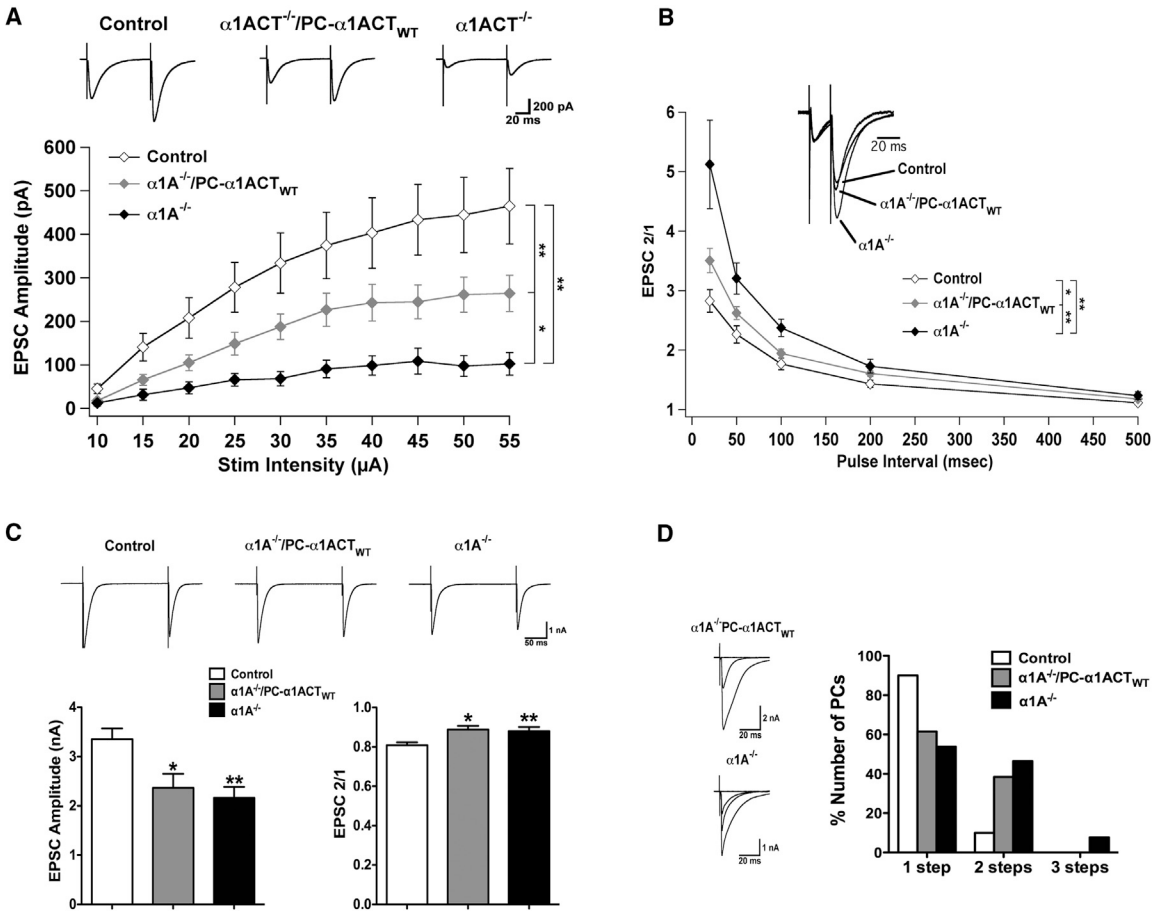

Figure 6. α1ACT Partially Restores PF-EPSC Amplitude but Does Not Affect CF Innervation or EPSC Properties

(A) PF-EPSC amplitude as a function of stimulus intensity for $\alpha 1A^{-/-}$ (n = 9, n = 4), $\alpha 1A^{-/-}$/PC-α1ACT (n = 16, n = 6), and WT (n = 11, n = 3) mice. Top: Typical PF-EPSCs at a stimulus intensity of 45 μA.

(B) Paired-pulse ratios as a function of stimulus interval in $\alpha 1A^{-/-}$, $\alpha 1A^{-/-}$/PC-α1ACT, and WT mice. Inset shows an overlay of representative traces from all three groups of mice with an interstimulus interval of 20 ms. EPSC1 from $\alpha 1A^{-/-}$/PC-α1ACT and WT mice were scaled to match the amplitude of EPSC1 from the $\alpha 1A^{-/-}$ mouse to facilitate comparison.

(C) Top: Representative CF-EPSCs elicited while holding at −30 mV. Bottom left: CF-EPSC amplitudes for $\alpha 1A^{-/-}$ (n = 10, n = 3), $\alpha 1A^{-/-}$/PC-α1ACT (n = 11, n = 3), and WT (n = 8, n = 3) mice. Bottom right: Paired-pulse depression of CF-EPSCs with 200 ms stimulus interval.

(D) Left: Representative traces from PCs in $\alpha 1A^{-/-}$ and $\alpha 1A^{-/-}$/PC-α1ACT mice exhibiting multiple CF innervation. Right: Percentage of PCs exhibiting one, two, or three discrete CF steps in $\alpha 1A^{-/-}$ (two steps: 6/13, three steps: 1/13, n = 3), $\alpha 1A^{-/-}$/PC-α1ACT (two steps: 5/13, n = 3), and WT (two steps: 1/9, n = 3) mice. All mice were age P16–P18. *p < 0.05, **p < 0.01. Data are mean ± SEM.

to the importance of P/Q-type Ca^{2+} channel function to neurotransmitter release at PF-PC synapses (Mintz et al., 1995). α1ACT expression also resulted in a partial reduction of PPRs at this synapse, which was surprising as PPRs generally reflect presynaptic release probabilities, and α1ACT is present only postsynaptically in $\alpha 1A^{-/-}$/PC-$\alpha 1ACT_{WT}$ mice, indicating that

(D) The lifespan of $\alpha 1A^{-/-}$/PC-$\alpha 1ACT_{WT}$ mice was significantly improved compared to $\alpha 1A^{-/-}$ (*p < 0.05). Some pups survived until age of P30 (n = 2, not included in the figure), whereas all $\alpha 1A^{-/-}$ pups died before P20.

(E–H) α1ACT expression improves cerebellar cortex and PC dendrites. Low power images of cerebellar ML (E). PC dendrites are labeled for calbindin-28 kDa (green). The thickness of the ML (F), the relative height of dendritic tree (G), and the density (as defined in the Experimental Procedures) of the PC dendritic tree (H) were reduced in $\alpha 1A^{-/-}$ mice and partially corrected in $\alpha 1A^{-/-}$/PC-$\alpha 1ACT_{WT}$ mice (100 dendritic trees from five mice at each group. Control is set as one, *p < 0.05).

(I) Immunolabeling of PFs and PC dendrites using anti-vGlut1 (red) and anti-calbindin (green) antibodies.

(J) Immunolabeling of CFs and PC dendrites using anti-vGlut2 (red) and anti-calbindin (green) antibodies.

(K and L) Quantitation of CF reach (K) and relative height of dendritic tree (L) (100 CFs, *p < 0.05). CF height was measured from the apical pole of PC somata to the tips of vGluT2-labeled CFs. Data are mean ± SEM.

See also Figure S5.

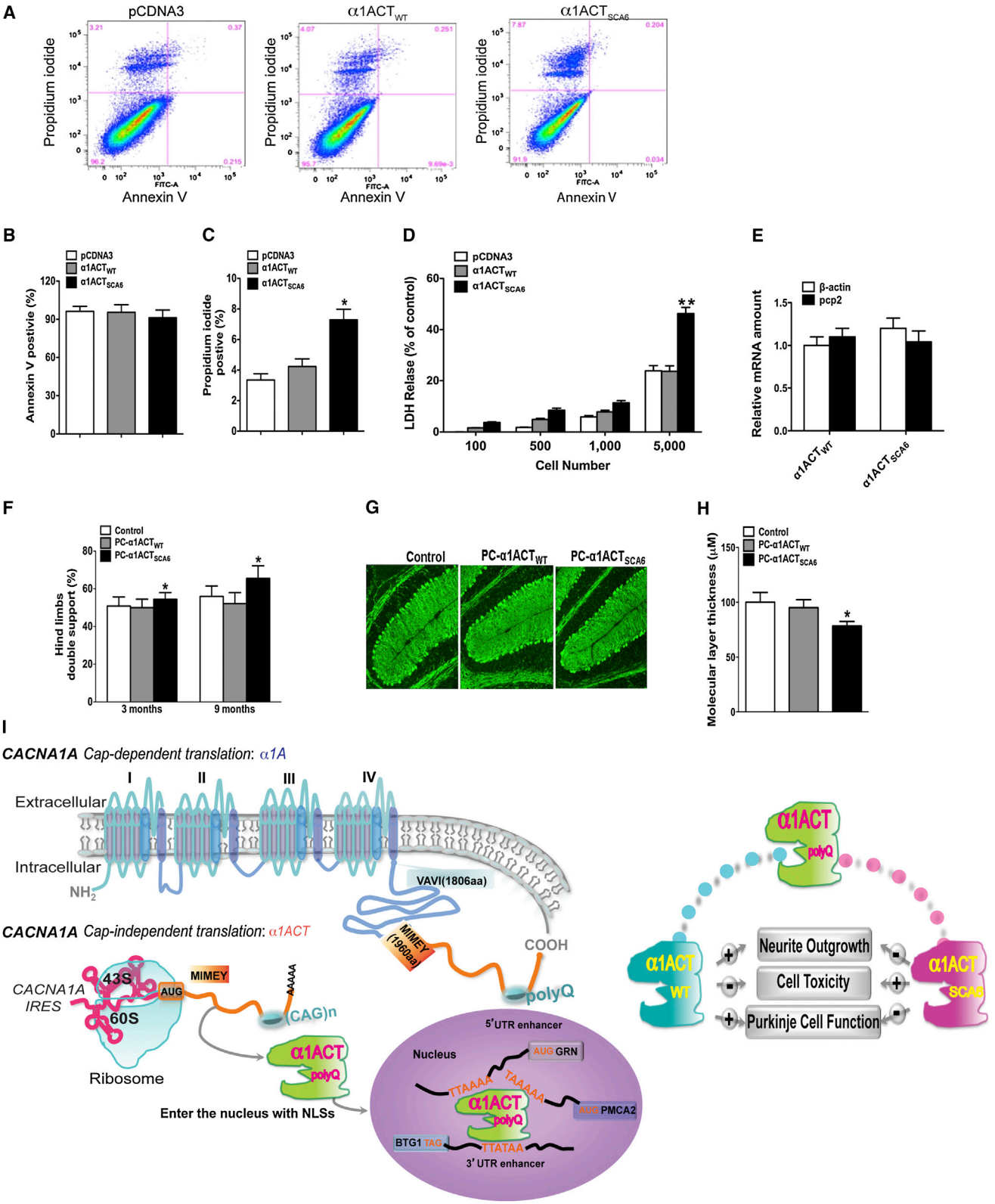

(legend on next page)

factors either directly or indirectly related to the postsynaptic target cell can also influence this parameter. Regardless, the residual elevation of PPRs in $\alpha 1A^{-/-}$/PC-α1ACT$_{WT}$ mice suggests that the incomplete restoration of PF-EPSC amplitude is due to a presynaptic deficit in these mice.

The absence of any discernable effect of α1ACT expression on CF-EPSCs indicates that actual P/Q-type Ca^{2+} channel function is required for the process of CF maturation, as has been suggested previously (Watanabe and Kano, 2011). Thus, it appears that the phenotypic benefits of α1ACT expression are due predominantly to the improvement in PF synaptic transmission.

α1ACT$_{SCA6}$ Abolishes the Normal Function of α1ACT in Gene Expression Regulation and Is Pathogenic In Vitro and In Vivo

Compared to the properties of the normal α1ACT protein, α1ACT$_{WT}$, bearing 4 or 11 glutamines, the α1ACT$_{SCA6}$ polypeptide had altered binding to the *BTG1* enhancer, showing additional DNA-protein complexes, and lacked the capacity to mediate expression via *BTG1* and *GRN* luciferase reporters and impaired expression of these genes in PC12 cells. α1ACT$_{SCA6}$ also failed to mediate neurite outgrowth when stably expressed in PC12 cells and caused increased cell death. This may explain why we did not obtain any mice with $\alpha 1A^{-/-}$/PC-α1ACT$_{SCA6}$ genotype. Mice overexpressing α1ACT$_{SCA6}$ on a normal background exhibited subtle but clearly measurable defects in motor functioning. Computerized treadmill gait analysis demonstrated progressive gait impairment with an increase in double limb support, a compensatory reaction to instability during walking. With advanced age, α1ACT$_{SCA6}$ was associated with thinning of the cerebellar cortex. These mice have reduced levels of expression of *TAF1*, *GRN*, *BTG1*, and *PMCA2*, the targets of α1ACT, relative to endogenous PC transcripts. These studies suggest that, rather than arising from ion channel dysfunction, the pathogenesis of SCA6 more closely resembles the toxic gain-of-function mechanism of the polyQ disorders (La Spada et al., 1991; Palhan et al., 2005; Sopher et al., 2004). This is supported by the lack of disturbed Ca^{2+} channel function in two mouse knockin studies of the SCA6 mutation (Saegusa et al., 2007; Watase et al., 2008). If additional studies further support this Ca^{2+} channel-independent mechanism, the demonstration of selective translation based on an IRES may pave the way for therapies targeted at suppressing the IRES function.

We have shown that the *CACNA1A* gene is bicistronic, encoding a newly identified transcription factor, α1ACT, involved with neurite outgrowth and PC maturation, within the α1A mRNA. α1ACT also bears the expanded polyQ tract in SCA6, which interrupts transcription factor function, impairs viability of cultured cells and is pathogenic in transgenic mice. These findings are summarized in the diagram in Figure 7I.

EXPERIMENTAL PROCEDURES

Materials and Standard Protocols

Cells, animals/mouse strains, antibodies, plasmids, and other materials are described in the Extended Experimental Procedures. The detailed protocols used for ChIP, ChIP-based cloning, ChIP quantitative real-time PCR, EMSA, luciferase assays, immunoprecipitation, immunohistochemistry, immunoblotting, quantitative real-time PCR, electrophysiology, and LDH assay are outlined in the Extended Experimental Procedures. This study involves specimens from human subjects and was approved by the Institutional Review Board of the University of Chicago Medical Center. All animal experiments were approved and carried out in accordance with the regulations and guidelines for the care and use of experimental animals at the Institutional Animal Care and Use Committee of the University of Chicago.

Protein Purification and Mass Spectrometry

Protein extracts from HEK293 cells stably transfected with α1A subunit bearing a Q11 allele were separated via anion exchange chromatography (HisTrap FF column) and further purified by ANTI-FLAG M2 affinity purification. α1ACT$_{WT}$ fragment protein in SDS-PAGE gel was digested in-gel with trypsin, and the resulting peptides were then analyzed via LC-MS/MS on an LTQ-Velos-Orbitrap mass spectrometer. See details in the Extended Experimental Procedures.

Immunohistochemistry and Microscopy

Detailed procedures of immunohistochemistry, antibodies, and dilutions are described in the Extended Experimental Procedures. PC12 cells were imaged 0, 24, 48, and 72 hr after NGF 24 hr treatment. Neurites were defined as processes longer than the width of the cell body. For each experiment, cells were imaged. Dendrites were analyzed by employing ImageJ and NeuroJ programs.

SUPPLEMENTAL INFORMATION

Supplemental Information includes Extended Experimental Procedures, six figures, four tables, and three movies and can be found with this article online at http://dx.doi.org/10.1016/j.cell.2013.05.059.

ACKNOWLEDGMENTS

We thank Professors Sangram S. Sisodia, Brian Popko, and Bert L. Semler for helpful comments on the manuscript, Dr. Raymond Roos for helpful discussions, Dr. Xiaorong Zhu for protein purification technical assistance, Dr. Jeremy Marks and Dr. Janice Wang for rat granule cell cultures and transfection, Dr. Yuanxin Hu for assembling the vectors for PC-α1ACT$_{WT}$ and PC-α1ACT$_{SCA6}$ mice and performing pilot immunoblot and immunohistochemical studies, Devon Collins and Kareisha Robinson for technical support in mouse breeding, genotyping, and DigiGait testing, and Tom Hampton for DigiGait

Figure 7. α1ACT$_{SCA6}$ Is a Pathogenic Fragment

(A) Representative fluorescence dot blots of FITC-Annexin-V- and propidium iodide (PI)-stained PC12 cells with stably transfected pcDNA3-FLAG, α1ACT$_{WT}$-FLAG, and α1ACT$_{SCA6}$-FLAG.

(B and C) Quantitation of Annexin-V- and PI-positive cells (*$p < 0.05$).

(D) Cell death as measured by LDH release assay (*$p < 0.05$).

(E) Expression levels of α1ACT$_{WT}$ and α1ACT$_{SCA6}$ in cerebellar homogenates by quantitative real-time PCR.

(F) Double support of hind paw was impaired in PC-α1ACT$_{SCA6}$ transgenic mice compared with PC-α1ACT$_{WT}$ transgenic mice at 3 and 9 months of age (**$p < 0.01$).

(G and H) Cerebellar cortical atrophy in PC-α1ACT$_{SCA6}$ transgenic mice. Low power images of cerebellar ML in mice at 20–26 months old (G) and quantitation of ML thickness (H) (*$p < 0.05$). PCs dendrites are labeled for calbindin (green).

(I) Schematic illustration of expression regulation and function of α1ACT. Data are mean ± SEM.

See also Figure S6.

assistance on data analysis. We also thank Professor Anne Willis for providing pRF vector, Dr. Suneil Malik for providing pGL3GRN vector, and Dr. Haiteng Deng for performing LC-MS/MS. We thank the Floyd family for supporting SCA6 research. This work was also supported by funding from the National Ataxia Foundation (NAF), the National Organization of Rare Diseases (NORD), and the National Institute of Neurological Disorders and Stroke (NS-062771) (to C.H.).

Received: August 9, 2012
Revised: February 5, 2013
Accepted: May 31, 2013
Published: July 3, 2013

REFERENCES

Baird, S.D., Turcotte, M., Korneluk, R.G., and Holcik, M. (2006). Searching for IRES. RNA *12*, 1755–1785.

Baker, M., Mackenzie, I.R., Pickering-Brown, S.M., Gass, J., Rademakers, R., Lindholm, C., Snowden, J., Adamson, J., Sadovnick, A.D., Rollinson, S., et al. (2006). Mutations in progranulin cause tau-negative frontotemporal dementia linked to chromosome 17. Nature *442*, 916–919.

Berthet, C., Guehenneux, F., Revol, V., Samarut, C., Lukaszewicz, A., Dehay, C., Dumontet, C., Magaud, J.P., and Rouault, J.P. (2002). Interaction of PRMT1 with BTG/TOB proteins in cell signalling: molecular analysis and functional aspects. Genes Cells *7*, 29–39.

Cain, S.M., and Snutch, T.P. (2011). Voltage-gated calcium channels and disease. Biofactors *37*, 197–205.

Catterall, W.A. (2011). Voltage-gated calcium channels. Cold Spring Harb. Perspect. Biol. *3*, a003947.

Cimato, T.R., Ettinger, M.J., Zhou, X., and Aletta, J.M. (1997). Nerve growth factor-specific regulation of protein methylation during neuronal differentiation of PC12 cells. J. Cell Biol. *138*, 1089–1103.

Coldwell, M.J., deSchoolmeester, M.L., Fraser, G.A., Pickering, B.M., Packham, G., and Willis, A.E. (2001). The p36 isoform of BAG-1 is translated by internal ribosome entry following heat shock. Oncogene *20*, 4095–4100.

Cornelis, S., Bruynooghe, Y., Denecker, G., Van Huffel, S., Tinton, S., and Beyaert, R. (2000). Identification and characterization of a novel cell cycle-regulated internal ribosome entry site. Mol. Cell *5*, 597–605.

Cruts, M., Gijselinck, I., van der Zee, J., Engelborghs, S., Wils, H., Pirici, D., Rademakers, R., Vandenberghe, R., Dermaut, B., Martin, J.J., et al. (2006). Null mutations in progranulin cause ubiquitin-positive frontotemporal dementia linked to chromosome 17q21. Nature *442*, 920–924.

Du, X., Rosenfield, R.L., and Qin, K. (2009). KLF15 is a transcriptional regulator of the human 17beta-hydroxysteroid dehydrogenase type 5 gene. A potential link between regulation of testosterone production and fat stores in women. J. Clin. Endocrinol. Metab. *94*, 2594–2601.

Fitzgerald, K.D., and Semler, B.L. (2009). Bridging IRES elements in mRNAs to the eukaryotic translation apparatus. Biochim. Biophys. Acta *1789*, 518–528.

Gomez-Ospina, N., Tsuruta, F., Barreto-Chang, O., Hu, L., and Dolmetsch, R. (2006). The C terminus of the L-type voltage-gated calcium channel Ca(V)1.2 encodes a transcription factor. Cell *127*, 591–606.

Hashimoto, K., and Kano, M. (2005). Postnatal development and synapse elimination of climbing fiber to Purkinje cell projection in the cerebellum. Neurosci. Res. *53*, 221–228.

Hashimoto, K., Tsujita, M., Miyazaki, T., Kitamura, K., Yamazaki, M., Shin, H.S., Watanabe, M., Sakimura, K., and Kano, M. (2011). Postsynaptic P/Q-type Ca2+ channel in Purkinje cell mediates synaptic competition and elimination in developing cerebellum. Proc. Natl. Acad. Sci. USA *108*, 9987–9992.

Ishiguro, T., Ishikawa, K., Takahashi, M., Obayashi, M., Amino, T., Sato, N., Sakamoto, M., Fujigasaki, H., Tsuruta, F., Dolmetsch, R., et al. (2010). The carboxy-terminal fragment of alpha(1A) calcium channel preferentially aggregates in the cytoplasm of human spinocerebellar ataxia type 6 Purkinje cells. Acta Neuropathol. *119*, 447–464.

Jun, K., Piedras-Rentería, E.S., Smith, S.M., Wheeler, D.B., Lee, S.B., Lee, T.G., Chin, H., Adams, M.E., Scheller, R.H., Tsien, R.W., and Shin, H.S. (1999). Ablation of P/Q-type Ca(2+) channel currents, altered synaptic transmission, and progressive ataxia in mice lacking the alpha(1A)-subunit. Proc. Natl. Acad. Sci. USA *96*, 15245–15250.

Koopman, G., Reutelingsperger, C.P., Kuijten, G.A., Keehnen, R.M., Pals, S.T., and van Oers, M.H. (1994). Annexin V for flow cytometric detection of phosphatidylserine expression on B cells undergoing apoptosis. Blood *84*, 1415–1420.

Kordasiewicz, H.B., Thompson, R.M., Clark, H.B., and Gomez, C.M. (2006). C-termini of P/Q-type Ca2+ channel alpha1A subunits translocate to nuclei and promote polyglutamine-mediated toxicity. Hum. Mol. Genet. *15*, 1587–1599.

Kozel, P.J., Friedman, R.A., Erway, L.C., Yamoah, E.N., Liu, L.H., Riddle, T., Duffy, J.J., Doetschman, T., Miller, M.L., Cardell, E.L., and Shull, G.E. (1998). Balance and hearing deficits in mice with a null mutation in the gene encoding plasma membrane Ca2+-ATPase isoform 2. J. Biol. Chem. *273*, 18693–18696.

Kubodera, T., Yokota, T., Ohwada, K., Ishikawa, K., Miura, H., Matsuoka, T., and Mizusawa, H. (2003). Proteolytic cleavage and cellular toxicity of the human alpha1A calcium channel in spinocerebellar ataxia type 6. Neurosci. Lett. *341*, 74–78.

Kurnellas, M.P., Lee, A.K., Szczepanowski, K., and Elkabes, S. (2007). Role of plasma membrane calcium ATPase isoform 2 in neuronal function in the cerebellum and spinal cord. Ann. N Y Acad. Sci. *1099*, 287–291.

La Spada, A.R., Wilson, E.M., Lubahn, D.B., Harding, A.E., and Fischbeck, K.H. (1991). Androgen receptor gene mutations in X-linked spinal and bulbar muscular atrophy. Nature *352*, 77–79.

Liu, S., and Friel, D.D. (2008). Impact of the leaner P/Q-type Ca2+ channel mutation on excitatory synaptic transmission in cerebellar Purkinje cells. J. Physiol. *586*, 4501–4515.

Marquèze-Pouey, B., Martin-Moutot, N., Sakkou-Norton, M., Lévêque, C., Ji, Y., Cornet, V., Hsiao, W.L., and Seagar, M. (2008). Toxicity and endocytosis of spinocerebellar ataxia type 6 polyglutamine domains: role of myosin IIb. Traffic *9*, 1088–1100.

Matsukawa, H., Wolf, A.M., Matsushita, S., Joho, R.H., and Knöpfel, T. (2003). Motor dysfunction and altered synaptic transmission at the parallel fiber-Purkinje cell synapse in mice lacking potassium channels Kv3.1 and Kv3.3. J. Neurosci. *23*, 7677–7684.

Matsushita, K., Wakamori, M., Rhyu, I.J., Arii, T., Oda, S., Mori, Y., and Imoto, K. (2002). Bidirectional alterations in cerebellar synaptic transmission of tottering and rolling Ca2+ channel mutant mice. J. Neurosci. *22*, 4388–4398.

Mintz, I.M., Sabatini, B.L., and Regehr, W.G. (1995). Calcium control of transmitter release at a cerebellar synapse. Neuron *15*, 675–688.

Palhan, V.B., Chen, S., Peng, G.H., Tjernberg, A., Gamper, A.M., Fan, Y., Chait, B.T., La Spada, A.R., and Roeder, R.G. (2005). Polyglutamine-expanded ataxin-7 inhibits STAGA histone acetyltransferase activity to produce retinal degeneration. Proc. Natl. Acad. Sci. USA *102*, 8472–8477.

Palmenberg, A.C., and Sgro, J.Y. (1997). Topological organization of picornaviral genomes: statistical prediction of RNA structural signals. Semin. Virol. *8*, 231–241.

Rajakulendran, S., Kaski, D., and Hanna, M.G. (2012). Neuronal P/Q-type calcium channel dysfunction in inherited disorders of the CNS. Nat. Rev. Neurol. *8*, 86–96.

Rouault, J.P., Samarut, C., Duret, L., Tessa, C., Samarut, J., and Magaud, J.P. (1993). Sequence analysis reveals that the BTG1 anti-proliferative gene is conserved throughout evolution in its coding and 3′ non-coding regions. Gene *129*, 303–306.

Saegusa, H., Wakamori, M., Matsuda, Y., Wang, J., Mori, Y., Zong, S., and Tanabe, T. (2007). Properties of human Cav2.1 channel with a spinocerebellar ataxia type 6 mutation expressed in Purkinje cells. Mol. Cell. Neurosci. *34*, 261–270.

Scott, V.E., Felix, R., Arikkath, J., and Campbell, K.P. (1998). Evidence for a 95 kDa short form of the alpha1A subunit associated with the omega-

conotoxin MVIIC receptor of the P/Q-type Ca2+ channels. J. Neurosci. *18*, 641–647.

Sopher, B.L., Thomas, P.S., Jr., LaFevre-Bernt, M.A., Holm, I.E., Wilke, S.A., Ware, C.B., Jin, L.W., Libby, R.T., Ellerby, L.M., and La Spada, A.R. (2004). Androgen receptor YAC transgenic mice recapitulate SBMA motor neuronopathy and implicate VEGF164 in the motor neuron degeneration. Neuron *41*, 687–699.

Spriggs, K.A., Stoneley, M., Bushell, M., and Willis, A.E. (2008). Re-programming of translation following cell stress allows IRES-mediated translation to predominate. Biol. Cell *100*, 27–38.

Spriggs, K.A., Cobbold, L.C., Ridley, S.H., Coldwell, M., Bottley, A., Bushell, M., Willis, A.E., and Siddle, K. (2009). The human insulin receptor mRNA contains a functional internal ribosome entry segment. Nucleic Acids Res. *37*, 5881–5893.

Stolze, H., Klebe, S., Petersen, G., Raethjen, J., Wenzelburger, R., Witt, K., and Deuschl, G. (2002). Typical features of cerebellar ataxic gait. J. Neurol. Neurosurg. Psychiatry *73*, 310–312.

Ul-Hussain, M., Zoidl, G., Klooster, J., Kamermans, M., and Dermietzel, R. (2008). IRES-mediated translation of the carboxy-terminal domain of the horizontal cell specific connexin Cx55.5 in vivo and in vitro. BMC Mol. Biol. *9*, 52.

Van Damme, P., Van Hoecke, A., Lambrechts, D., Vanacker, P., Bogaert, E., van Swieten, J., Carmeliet, P., Van Den Bosch, L., and Robberecht, W. (2008). Progranulin functions as a neurotrophic factor to regulate neurite outgrowth and enhance neuronal survival. J. Cell Biol. *181*, 37–41.

Watanabe, M., and Kano, M. (2011). Climbing fiber synapse elimination in cerebellar Purkinje cells. Eur. J. Neurosci. *34*, 1697–1710.

Watase, K., Barrett, C.F., Miyazaki, T., Ishiguro, T., Ishikawa, K., Hu, Y., Unno, T., Sun, Y., Kasai, S., Watanabe, M., et al. (2008). Spinocerebellar ataxia type 6 knockin mice develop a progressive neuronal dysfunction with age-dependent accumulation of mutant CaV2.1 channels. Proc. Natl. Acad. Sci. USA *105*, 11987–11992.

Wilkins, M.R., Gasteiger, E., Bairoch, A., Sanchez, J.C., Williams, K.L., Appel, R.D., and Hochstrasser, D.F. (1999). Protein identification and analysis tools in the ExPASy server. Methods Mol. Biol. *112*, 531–552.

Wilson, J.E., Powell, M.J., Hoover, S.E., and Sarnow, P. (2000). Naturally occurring dicistronic cricket paralysis virus RNA is regulated by two internal ribosome entry sites. Mol. Cell. Biol. *20*, 4990–4999.

Zacharias, D.A., and Kappen, C. (1999). Developmental expression of the four plasma membrane calcium ATPase (Pmca) genes in the mouse. Biochim. Biophys. Acta *1428*, 397–405.

Zhuchenko, O., Bailey, J., Bonnen, P., Ashizawa, T., Stockton, D.W., Amos, C., Dobyns, W.B., Subramony, S.H., Zoghbi, H.Y., and Lee, C.C. (1997). Autosomal dominant cerebellar ataxia (SCA6) associated with small polyglutamine expansions in the alpha 1A-voltage-dependent calcium channel. Nat. Genet. *15*, 62–69.

Zu, T., Duvick, L.A., Kaytor, M.D., Berlinger, M.S., Zoghbi, H.Y., Clark, H.B., and Orr, H.T. (2004). Recovery from polyglutamine-induced neurodegeneration in conditional SCA1 transgenic mice. J. Neurosci. *24*, 8853–8861.

Zucker, R.S., and Regehr, W.G. (2002). Short-term synaptic plasticity. Annu. Rev. Physiol. *64*, 355–405.

Zuker, M. (2003). Mfold web server for nucleic acid folding and hybridization prediction. Nucleic Acids Res. *31*, 3406–3415.